Investigations on RF Behavior of a V-Band Second Harmonic Gyrotron for 100/200 kW Operation

Surbhi Adya, *Graduate Student Member, IEEE*, S. Yuvaraj, Meenakshi Rawat, *Member, IEEE*, M. V. Kartikeyan, *Fellow, IEEE*, M. K. Thumm, *Life Fellow, IEEE*

***Abstract*—This paper presents the investigations on RF-behavioral aspects for the possible operation of a V-band, continuous wave (CW) second harmonic gyrotron for plasma diagnostic application. Keeping in view the design goals and constraints, initial design studies for the mode selection and the computation of starting currents are carried out. From these studies, two possible modes, namely, $TE_{7,3}$ and $TE_{8,3}$ are considered for second harmonic operation. Later, the cold cavity design and self-consistent calculations are carried out for the selected operating modes. All the computations are performed using a latest version of our in-house code Gyrotron Design Studio Second Harmonic Version 2020 (GDS2H-2020) with Glidcop as the cavity material. The RF behavior studies confirm the feasible operation of such a second harmonic gyrotron with power levels in excess of 115.52/217.64 kW with the chosen modes of operation.**

***Index Terms*—Cold cavity calculations, Mode competition, Plasma diagnostics, Second harmonic gyrotrons, Single-mode self-consistent computations.**

I. Introduction

GYROTRONS are powerful radiation sources capable of producing very high powers ($\approx 10^3 - 10^6$ W) at electron cyclotron frequency or its harmonics, ranging from microwave to millimetric wavelengths. It has widened the mm-wave band of the electromagnetic spectrum for high-power applications. These devices are mainly used for electron cyclotron resonance heating (ECRH) and stabilization of plasmas in controlled thermonuclear fusion research (CFTR) experiments, also, have potential applications in industrial or technological heating problems [1], [2]. Plasma diagnostics in the millimeter and sub-millimeter wave ranges are beneficial for determining the plasma density, electron temperatures, the direction of the magnetic field, and non-thermal fluctuations. For the ECRH of plasmas, one needs gyrotrons capable of delivering greater than a megawatt CW power at frequencies around 170-300 GHz depending on the configuration of the fusion reactor. The efforts have resulted in an increase of output power as well as the efficiency of gyrotrons which has been shown over the years [2]. The demonstration of a 28 GHz fundamental gyrotron at 200 kW was done in 1980 [3] and their scaled versions led to the development of 60 GHz gyrotrons for the same power level both in pulsed and CW operation [4]. Gyrotrons operating at fundamental harmonic ranging from 28-70 GHz with output powers of several kilowatts for ECRH applications have been published [5], [6]. The authors have reported articles on a series of fundamental gyrotrons at 42 GHz, 60 GHz, 84 GHz, and 95 GHz with output power levels from 100-500 kW for ECRH in Tokamak and Industrial, Scientific and Medical (ISM) applications [7]-[11]. Other than the fundamental gyrotrons, substantial research work has been carried out on second harmonic gyrotrons at 95 GHz [12].

The specific advantage of second harmonic gyrotrons operating at a given frequency is the requirement that the magnetic field will be reduced by half, but at the cost of efficiency as compared to the fundamental operation. The reduction in the magnetic field of the gyrotron leads to the reduction in the size of the superconducting magnetic coils and the associated cooling systems. Thus, the overall volume of the second harmonic gyrotron is greatly reduced in comparison with a first harmonic gyrotron and thereby reduces the overall space and maintenance cost of the system. However, such gyrotrons are very useful for low-cost and compact applications [13]. Investigations on second harmonic gyrotrons (s = 2) for producing CW powers around 25-50 kW to 200 kW at frequencies of 24 GHz and 42 GHz respectively for ISM and Tokamak applications were reported in [14], [15]. Similarly, second harmonic gyrotrons at 28 GHz with 10 kW of output power were developed for electron cyclotron resonance ion sources [16] and with 20 kW power for the evaluation of emitter technologies [17]. Also, a second harmonic gyrotron with 50 kW power at 95 GHz for ISM applications has been developed at Ariel University [18]. Studies on specific gyrotrons for plasma diagnostics were reported in [5], [6], [8]. Recent progress on the state-of-the-art development of gyrotrons and allied sources are periodically reported in [2].

There is a specific requirement for a compact second harmonic gyrotron with output power ≈ 100-200 kW, CW, for plasma diagnostic applications in an experimental Tokamak in India. This gives the motivation to take up the critical design and assessment of such a high power source. The challenge in this objective is to design the gyrotron (common input system, interaction cavity and output system) which can support dual power operation (100/200 kW) at V-band. After considering these design objectives, the electrical design is carried out by considering two cavity modes. The advantage

Surbhi Adya, Meenakshi Rawat and M. V. Kartikeyan are with the Department of Electronics and Communication Engineering, Indian Institute of Technology, Roorkee, Uttarakhand, 247667, India. Presently, M. V. Kartikeyan is on deputation with the Department of Electrical Engineering, Indian Institute of Technology, Tirupati, Andhra Pradesh, 517506, India. S. Yuvaraj is with Department of Electronics and Communication Engineering at National Institute of Technology, Tadepalligudem, Andhra Pradesh, 534101, India. M. K. Thumm is with Karlsruhe Institute of Technology, North Campus, Institut fuer Hochleistungsimpuls -und Mikrowellentechnik (IHM), Hermann von Helmholtzplatz 1, D-76344 Eggenstein-Leopoldshafen, Germany.
E-mail: sadya@ec.iitr.ac.in; kartik@ieee.org

Manuscript received XXXX XX, XXXX; revised XXXX XX, XXXX.

of this design over other reported works are that the chosen modes in this study can support dual power operation and the power levels in the second harmonic operations are increased towards 200 kW. In the present work, the feasibility studies and investigations on RF behavioral aspects leading to the electrical design of a second harmonic gyrotron capable of delivering 100 kW and 200 kW CW output powers operating at 60 GHz have been presented. Further, it has been planned to carry the design considering two probable operating modes with caustic radius of 0.423/0.45 that probably support a single and compatible output system. The paper is divided in four sections. A brief literature overview pertaining to the subject, motivation and organization of the paper are given in Section-I. Table I summarizes the design objectives and constraints of such a typical gyrotron. Mode competition and starting current computations are given in Section-II. These studies suggest two prominent modes, namely, $\mathrm{TE}_{7,3}$ and $\mathrm{TE}_{8,3}$ to realize such operation. The RF-behavioral aspects are presented in Section-III. These investigations comprise cold cavity design and single-mode self-consistent computations for output power and efficiencies under second harmonic operation for the selected operating modes. Glidcop with conductivity σ = 2.57 x 10^7 S/m [19] (deduction due to cavity heating and surface roughness) has been considered as cavity material for the design studies. By varying the nominal electron beam parameters, power and efficiencies are computed self-consistently to realize a second harmonic operation in a low power ($\approx 100\,\mathrm{kW}$) and a medium power ($\approx 200\,\mathrm{kW}$) regimes respectively for both the modes chosen for operation. An in-house built latest version of the computer code-package GDS2H-2020 has been used for these computations. Earlier versions of GDS2H were reported in [20], [21]. Finally conclusions are given in Section-IV.

TABLE I
DESIGN GOALS AND CONSTRAINTS OF THE PROPOSED SECOND-HARMONIC GYROTRON.

Frequency	60 GHz	60 GHz
Output Power	100 kW, CW	200 kW, CW
Diffractive Quality Factor	1500-2500	1500-2500
Electron Beam Voltage	52-58 kV	63-69 kV
Electron Beam Current	8-14 A	11-16 A
Magnetic Field at Cavity Center	1.1-1.3 T	1.1-1.3 T
Electron Beam Velocity Ratio	$\approx$ 1.40	$\approx$ 1.40
Total Output Efficiency	$>$ 20 %	$>$ 20 %
Estimated Cavity Wall Loading	$< 2\ \mathrm{kW/cm^2}$	$< 2\ \mathrm{kW/cm^2}$
Total Internal Losses	$<$ 8 %	$<$ 8 %

II. Mode Selection and Computation of Starting Currents

For the gyrotron to operate in the $\mathrm{TE}_{\mathrm{mp}}$ mode, the radius of the cavity R_0 is calculated using the expression $\chi_{m,p}\lambda/2\pi$ where the pth root of $J'_m(x)$ is $\chi_{m,p}$ and the free space wavelength corresponding to the operating frequency f_r is denoted by λ. Also, the radius of the electron beam, R_e is computed using the formula $\chi_{m\pm s,i}R_0/\chi_{m,p}$, where '$s$' denotes the harmonic number which is 2 here in the case of second harmonic gyrotrons (with i = 1 or 2 corresponding to first and second radial field maximum). The $\pm$ symbol after the mode indices implies counter-rotating (+) and co-rotating (-) modes. The co-rotating mode is considered since it offers better electron beam-field coupling. Considering the frequency of operation (at 60 GHz) and output power (100-200 kW), modes with eigenvalues between 8-20 are considered for the study of mode competition. Modes that support the same electron beam radius, second harmonic and fundamental neighbors, and modes with $m/\chi_{m,p} \approx 0.4 - 0.5$ that support an advanced dimpled wall launcher of the quasi-optical output coupler were considered for mode selection. Probable selected modes are listed along with other parameters in Tables II and III. From these computations, two promising modes, $\mathrm{TE}_{7,3}$ and $\mathrm{TE}_{8,3}$, are finally selected as operating modes. Further, these two modes have similar caustic radius (0.423/0.45) and a single output system can probably work for both the modes if designed and optimized accordingly.

TABLE II
AZIMUTHAL INDEX (m), RADIAL INDEX (p), HARMONIC (s), EIGENVALUE ($\chi m, p$), CAVITY RADIUS (R_0), ELECTRON BEAM RADIUS (R_e), AND RELATIVE CAUSTIC RADIUS ($m/\chi_{m,p}$) FOR THE PROBABLE MODES CONSIDERED FOR 100/200 KW SECOND HARMONIC GYROTRON. HERE, THE MAIN MODE IS $\mathrm{TE}_{7,3}$.

m	p	s	$\chi_{m,p}$	$R_0(mm)$	$R_e(mm)$	$\frac{m}{\chi_{m,p}}$
7	4	2	19.94185	15.877	5.107	0.351
7	**3**	**2**	**16.52937**	**13.160**	**5.107**	**0.423**
7	2	2	12.93239	10.296	5.107	0.541
8	3	2	17.77401	14.151	5.972	0.450
6	3	2	15.26818	12.156	4.233	0.392
4	4	2	15.96411	12.710	2.431	0.250
5	4	2	17.31284	13.784	3.344	0.288
6	4	2	18.63744	14.838	4.233	0.321
10	2	2	16.44785	13.095	7.680	0.60
0	5	2	16.47063	13.113	2.431	0
7	1	1	8.57784	13.658	11.865	0.816
3	2	1	8.01524	12.763	4.863	0.374
1	3	1	8.53632	13.592	6.101	0.117

After performing the initial mode selection calculations, starting currents were computed for these main modes considering all the probable competing modes. The starting currents, I_{start} provide a clear understanding of how the different modes are separated in the frequency domain. This also considers their coupling with the electron beam. The computation of the starting currents can be performed using a linearized single-mode theory in numerous ways, as reported in [1], [15], [22]-[25]. From earlier studies, it is clear that the electron beam-field coupling constant and the starting current are inversely proportional to each other as obtained from the expression $J^2_{m\pm s}(\chi_{m,p}R_e/R_0)/\pi(\chi^2_{m,p} - m^2)J^2_m(\chi_{m,p})$; and therefore, for a given mode, if the electron beam-field coupling constant is too small then, the value of I_{start} will be large and the mode will not oscillate [15].

The Fig. 1 and 2 depicts the starting currents as a function of the magnetic field which is determined independently for the two considered modes. Hence, due to the minimum starting current and less mode competition, $\mathrm{TE}_{7,3,-}$ and $\mathrm{TE}_{8,3,-}$ are selected as the operating modes.

TABLE III
AZIMUTHAL INDEX (m), RADIAL INDEX (p), HARMONIC (s), EIGENVALUE ($\chi m, p$), CAVITY RADIUS (R_0), ELECTRON BEAM RADIUS (R_e), AND RELATIVE CAUSTIC RADIUS ($m/\chi_{m,p}$) FOR THE PROBABLE MODES CONSIDERED FOR 100/200 KW SECOND HARMONIC GYROTRON. HERE, THE MAIN MODE IS $\mathrm{TE}_{8,3}$.

m	p	s	$\chi_{m,p}$	$R_0(mm)$	$R_e(mm)$	$\frac{m}{\chi_{m,p}}$
8	4	2	21.22906	16.902	5.972	0.376
8	**3**	**2**	**17.77401**	**14.151**	**5.972**	**0.450**
8	2	2	14.11552	11.238	5.972	0.566
9	3	2	19.00459	15.131	6.829	0.473
7	3	2	16.52937	13.160	5.107	0.423
5	4	2	17.31284	13.784	3.344	0.288
6	4	2	18.63744	14.838	4.233	0.321
7	4	2	19.94185	15.877	5.107	0.351
11	2	2	17.60027	14.012	8.527	0.624
3	5	2	17.78875	14.163	1.465	0.168
7	1	1	8.57784	13.658	11.865	0.816
8	1	1	9.64742	15.362	13.658	0.829
3	2	1	8.01524	12.763	4.863	0.374
4	2	1	9.28240	14.780	6.689	0.430
1	3	1	8.53632	13.592	6.101	0.117

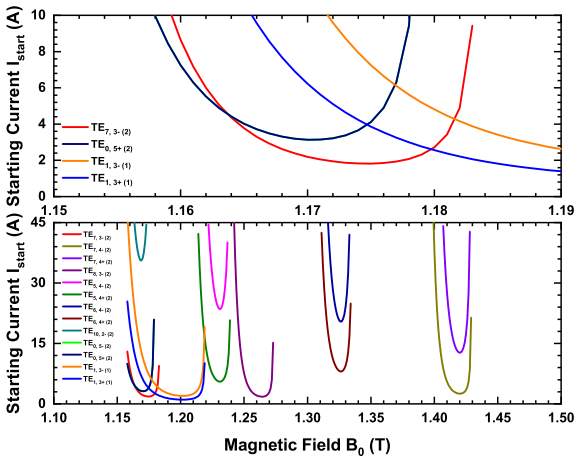

Fig. 1. Plot of starting current I_{start} as a function of magnetic field B_0 for different modes with electron beam radius (R_e) optimized for the $\mathrm{TE}^{(2)}_{7,3}$ mode. The indexes $\pm$ indicate counter-rotating (+) and co-rotating (-) modes. Electron beam voltage: U_b = 55 kV, Electron beam velocity ratio: α = 1.4, Cavity radius: R_0 = 13.16 mm and electron beam radius: R_e = 5.107 mm.

III. RF CAVITY DESIGN AND SELF-CONSISTENT COMPUTATIONS

The cold cavity design calculations are performed after an elaborate study of the cavity for optimizing its geometrical dimensions. The free-space wavelength corresponding to the operating frequency of 60 GHz is 5.0 mm. The RF interaction space comprises a typical cylindrical cavity with up and down tapers. It includes three sections, with the first one as the input down taper length designated by L_1 for preventing the back propagation of the RF power towards the electron gun side followed by the straight midsection length indicated by L_2 where beam-wave interaction occurs and L_3 is the length of the up taper that connects the interaction structure with the device output system. Also, θ_1 and θ_3 are their respective

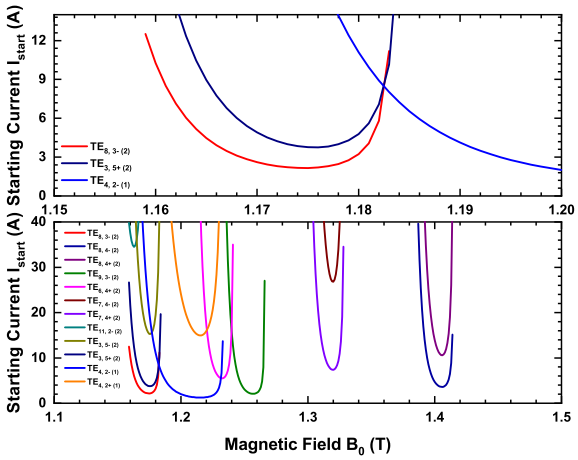

Fig. 2. Plot of starting current I_{start} as a function of magnetic field B_0 for different modes with electron beam radius (R_e) optimized for the $\mathrm{TE}^{(2)}_{8,3}$ mode. The indexes $\pm$ indicate counter-rotating (+) and co-rotating (-) modes. Beam voltage: U_b = 55 kV, Electron beam velocity ratio: α = 1.4, Cavity radius: R_0 = 14.15 mm and electron beam radius: R_e = 5.972 mm.

taper angles. Parabolic smoothing of the down and up tapers (with roundings denoted by D_1 and D_2) has been carried out to avoid unwanted mode conversion [1], [13]. The cavity radius for $\mathrm{TE}_{7,3}$ mode is 13.16 mm and for $\mathrm{TE}_{8,3}$ mode it is 14.15 mm. However, both the cavities are fixed at taper lengths of $L_1 = L_3 = 26$ mm with tapering angles θ_1/θ_3 = 3.0°/3.5° and the corresponding roundings at D_1/D_2 = 8.5/8.5 mm. By varying the mid-section length for both the modes, frequency and diffractive quality factors are computed and are tabulated in Table IV. In addition, cavity geometry and normalized field profile for both these modes has been appreciated in Fig. 3.

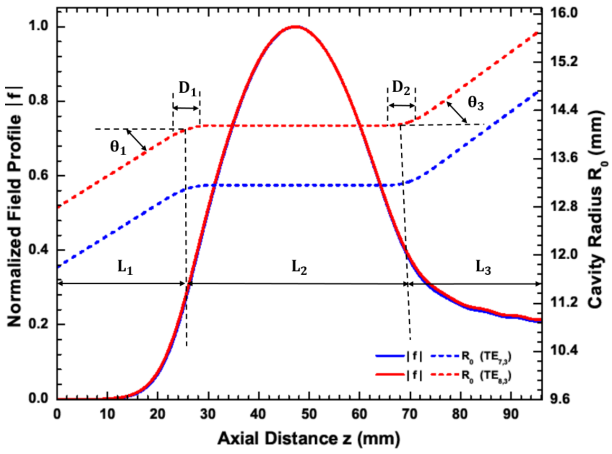

Fig. 3. Normalized field profile along geometry of the cavity for $\mathrm{TE}_{7,3}$ and $\mathrm{TE}_{8,3}$.

In the next step, cavity output power and efficiencies are computed self-consistently by suitably choosing the nominal electron beam parameters for second harmonic operation for both the modes considered. We have chosen two regimes of operation to work around at 100 kW and 200 kW of output powers respectively as required by the end-user to demonstrate a low-power and medium power operation with efficiency $> 20\%$. Power and efficiencies obtained for an optimized set

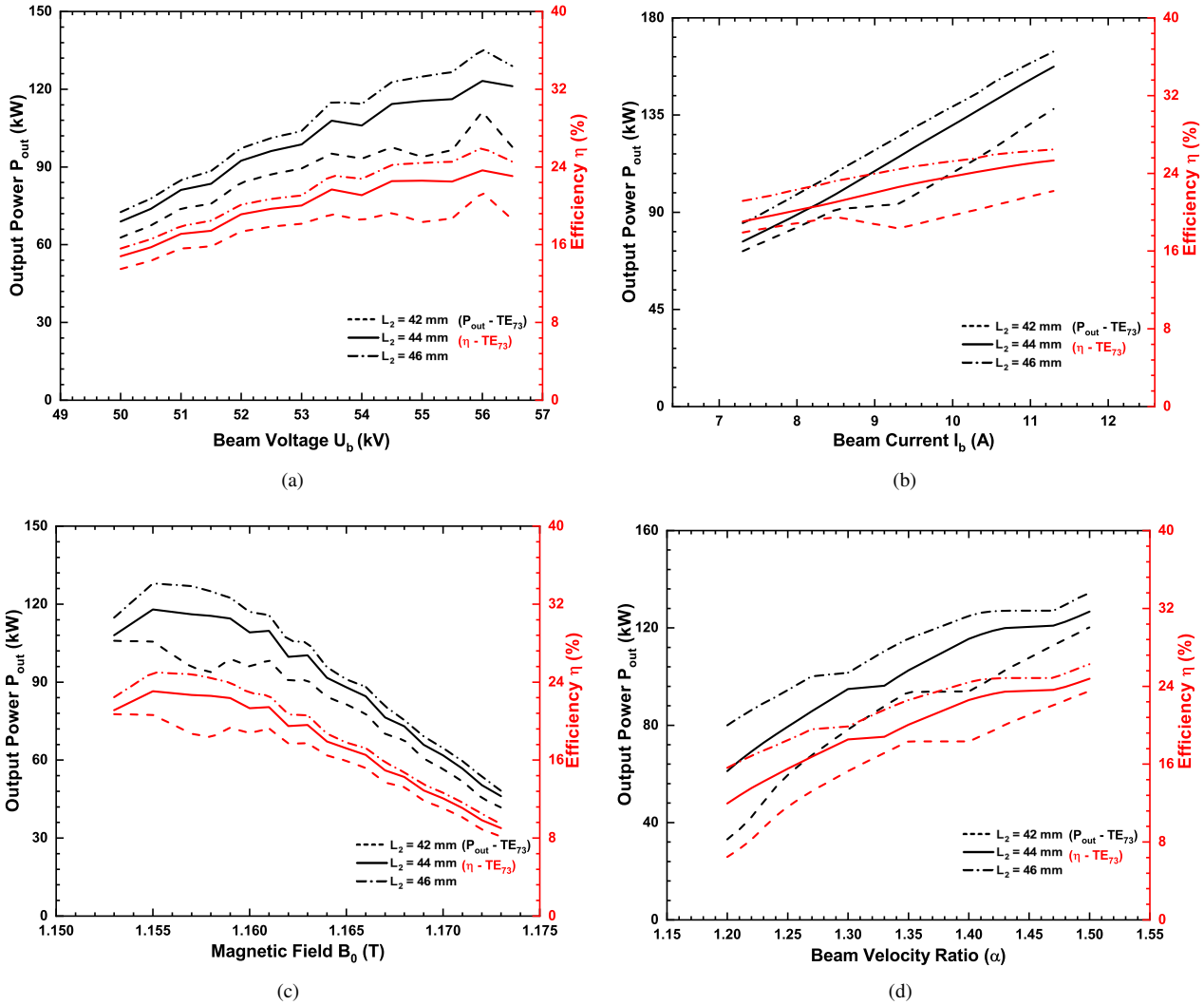

Fig. 4. Plots of output power and efficiency as functions of nominal electron beam parameters at different L_2 for the $TE_{7,3}$ operating mode - low power operation (a) U_b variation with I_b = 9.3 A, B_0 = 1.158 T, α = 1.4 (b) I_b variation with U_b = 55 kV, B_0 = 1.158 T, α = 1.4 (c) B_0 variation with U_b = 55 kV, I_b = 9.3 A, α = 1.4 (d) α variation with U_b = 55 kV, I_b = 9.3 A, B_0 = 1.158 T.

TABLE IV
FREQUENCY AND QUALITY FACTOR AS A FUNCTION OF THE MID-SECTION LENGTH OF THE CAVITY RESONATOR L_2 FOR THE OPERATING MODES.

Parameters	$TE_{7,3}$		$TE_{8,3}$	
L_2 (mm)	f (GHz)	Q_D	f (GHz)	Q_D
42	60.046	1602	60.050	1600
44	60.041	1804	60.044	1793
46	60.036	2021	60.039	2008

of nominal electron beam parameters along with the cavity geometry for both modes of operation are given in Table V. Glidcop with conductivity σ = 2.57 x 10^7 S/m is considered for these computations which accounts for a surface roughness of 1 μm at 250°C following [19]. As far the wall loading is concerned, both these modes tend to operate well within the limitation of 2 kW/cm^2 for Glidcop and one can produce a suitable transverse output coupling scheme effectively.

Useful parametric ana[sis] has been carried out by varying

TABLE V
SINGLE MODE SELF-CONSISTENT COMPUTATION RESULTS. THE CAVITY GEOMETRY ALSO GIVEN.

Parameters	$TE_{7,3}$	$TE_{8,3}$
$L_1/L_2/L_3$ (mm)	26/44/26	26/44/26
$\theta_1/\theta_2/\theta_3$ (°)	3.0/0/3.5	3.0/0/3.5
D_1/D_2 (mm)	8.5/8.5	8.5/8.5
R_0 (mm)	13.16	14.15
f (GHz)	60.041	60.044
Q_D	1804.00	1793.00
R_e (mm)	5.107	5.972
σ (S/m)	2.57 x 10^7	2.57 x 10^7
ρ_{wall} (kW/cm^2)	0.31/0.60	0.33/0.62
U_b (kV)	55/65	55/65
I_b (A)	9.3/12.2	11.8/14.7
α	1.4	1.4
B_0 (T)	1.158/1.173	1.159/1.174
η (%)	22.59/27.45	23.00/26.36
P_{out} (kW)	115.52/217.64	149.29/251.89

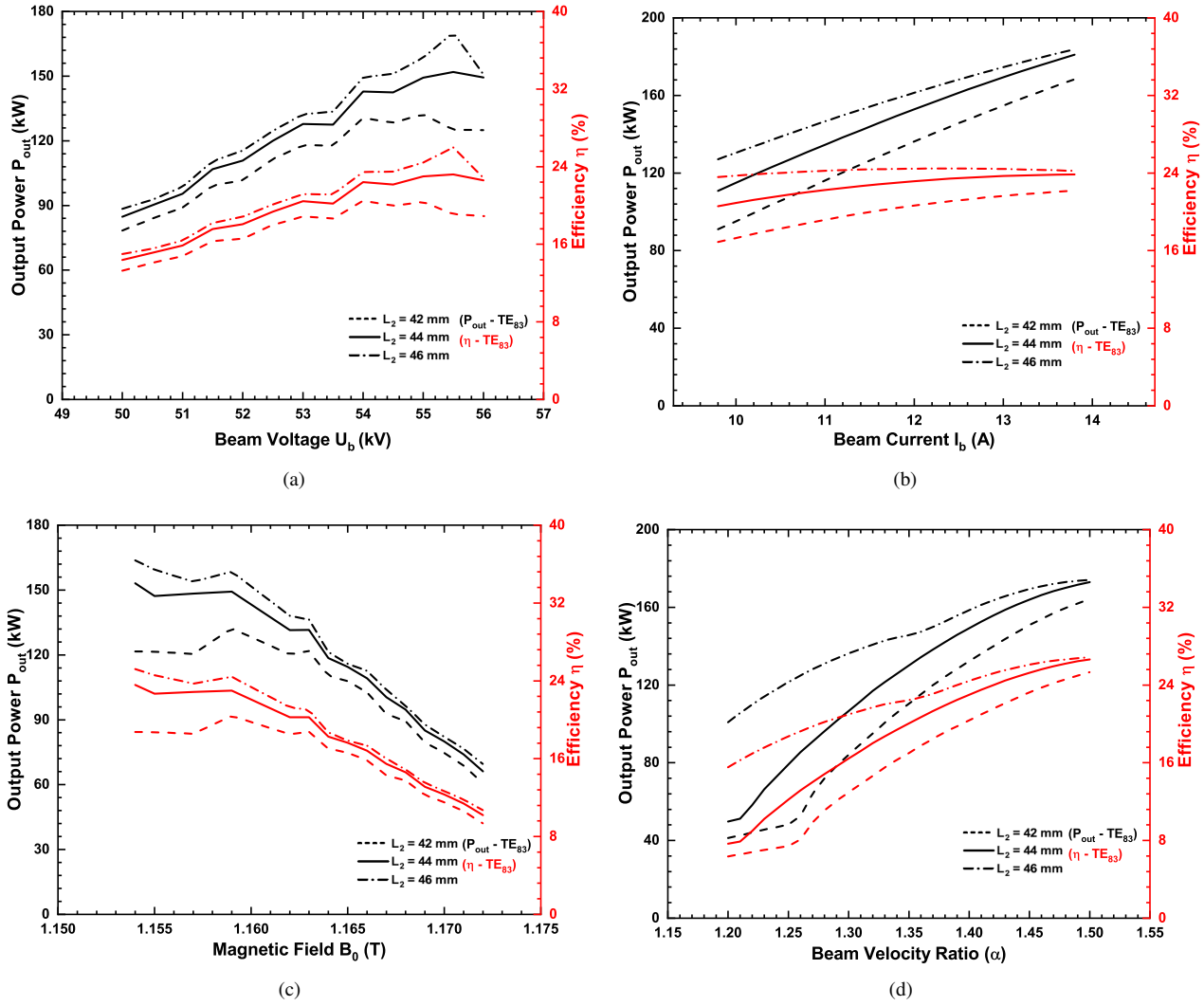

Fig. 5. Plots of output power and efficiency as functions of nominal electron beam parameters at different L_2 for the $TE_{8,3}$ operating mode - low power operation (a) U_b variation with I_b = 11.8 A, B_0 = 1.159 T, α = 1.4 (b) I_b variation with U_b = 55 kV, B_0 = 1.159 T, α = 1.4 (c) B_0 variation with U_b = 55 kV, I_b = 11.8 A, α = 1.4 (d) α variation with U_b = 55 kV, I_b = 11.8 A, B_0 = 1.159 T.

the nominal electron beam parameters and output power and efficiencies are computed and appreciated graphically as shown in Figs. 4, 5 and 6, 7 for both the low and medium power regimes, respectively. It can be observed from the Fig. 4 that with $TE_{7,3}$ mode, ≈120 kW of output power is obtained with 22.59% efficiency at L_2 = 44 mm with electron beam voltage U_b = 55 kV, electron beam current I_b = 9.3 A, magnetic field B_0 = 1.158 T and electron beam velocity ratio α = 1.4. Similarly, with $TE_{8,3}$ as the operating mode, ≈150 kW of output power is obtained with 23.00% efficiency with U_b = 55 kV, I_b = 11.8 A, B_0 = 1.159 T and α = 1.4 as shown in Fig. 5.

Similarly, for the medium power regime (as shown in Fig. 6), for $TE_{7,3}$ mode with L_2 = 44 mm and with U_b = 65 kV, I_b = 12.2 A, B_0 = 1.173 T and α = 1.4, an output power of ≈220 kW with an efficiency of 27.45% is achieved. Also, for the $TE_{8,3}$ mode with L_2 = 44 mm and with U_b = 65 kV, I_b = 14.7 A, B_0 = 1.174 T and α = 1.4, an output power of ≈250 kW with an efficiency of 26.16% is attained (as shown in Fig. 7). Similar calculations are also carried out for different mid section length of the cavity L_2 = 42/46 mm (see Figs. 4, 5, 6 and 7). All the computations in Section-II and Section-III are duly carried out using GDS2H-2020.

IV. Conclusion

A second harmonic gyrotron has been designed and investigated for the two modes $TE_{7,3}$ and $TE_{8,3}$ at 60 GHz. As the second harmonic operation requires nearly half of the magnetic field when compared with its fundamental counter part, it makes the system relatively compact and cost effective. Using an in-house code GDS2H-2020, mode selection calculations and starting current calculations have been computed for the selected modes. Further, cold cavity design and self-consistent computations have been carried out to study the RF behavioral aspects of this specific second harmonic gyrotron. Operating with $TE_{7,3}$ mode, the output power around 115.52 kW and 217.64 kW with efficiencies at 22.59% and 27.45% respectively have been obtained. Also, operating with $TE_{8,3}$

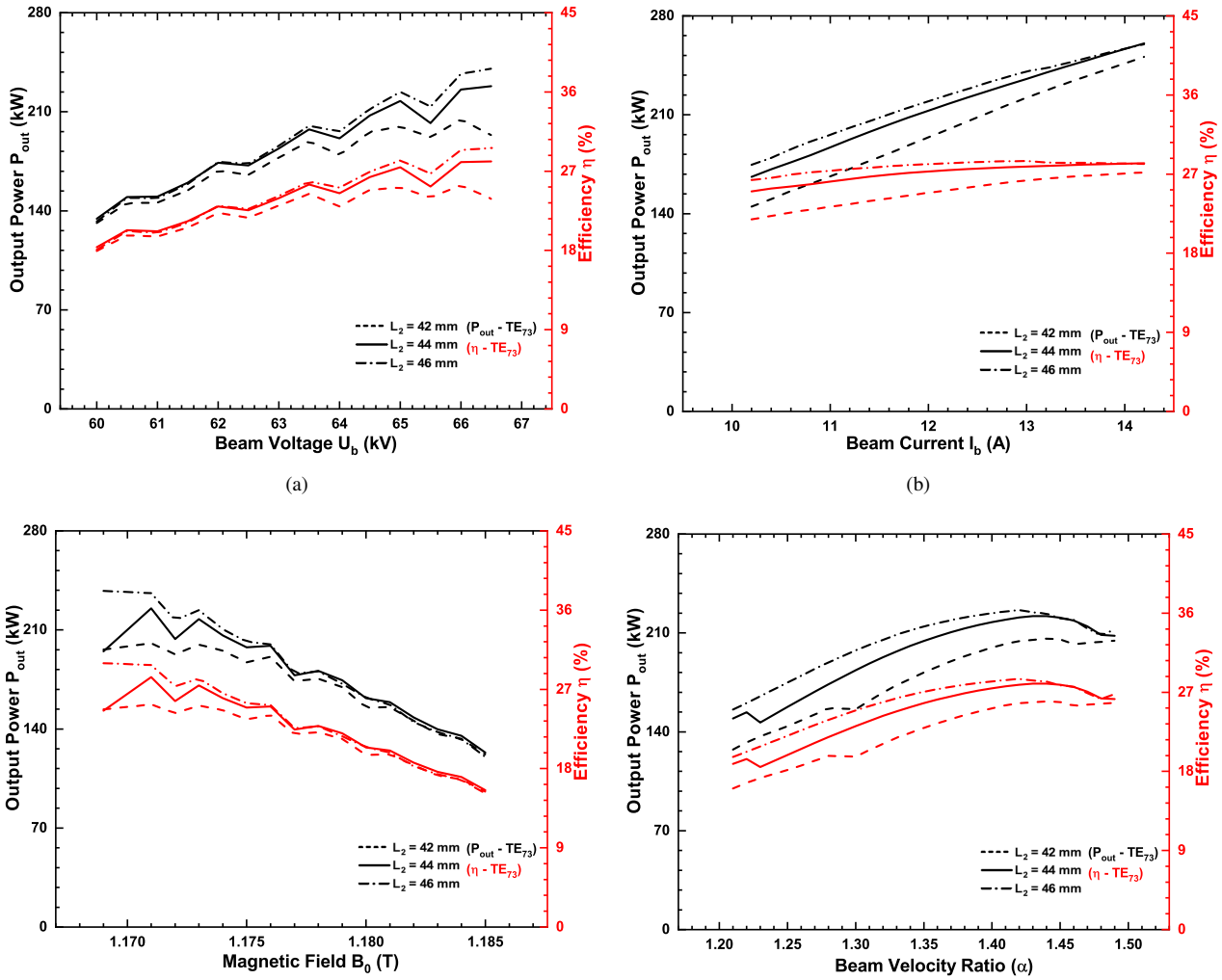

Fig. 6. Plots of output power and efficiency as functions of nominal electron beam parameters at different L_2 for the $TE_{7,3}$ operating mode - medium power operation (a) U_b variation with I_b = 12.2 A, B_0 = 1.173 T, α = 1.4 (b) I_b variation with U_b = 65 kV, B_0 = 1.173 T, α = 1.4 (c) B_0 variation with U_b = 65 kV, I_b = 12.2 A, α = 1.4 (d) α variation with U_b = 65 kV, B_0 = 1.173 T, I_b = 12.2 A.

mode, the output power around 149.29 kW and 251.89 kW with efficiencies at 23.00% and 26.36% have been attained. Therefore, both the modes proved their operational suitability at the desired power levels. However, higher output power levels have been achieved by operating the cavity with $TE_{8,3}$ mode without considerable variation in the ohmic wall loading as compared to $TE_{7,3}$ mode. The design studies of the input system with electron guns and magnet systems along with the quasi-optical output coupler and the dielectric output window for the proposed gyrotron are in progress at present.

REFERENCES

[1] M. V. Kartikeyan, E. Borie, and M. Thumm, *Gyrotrons: High Power Microwave and Millimeter Wave Technology,* Berlin-Heidelberg, Germany: Springer-Verlag, 2004.

[2] Manfred Thumm, "State-of-the-art of high power gyro-devices and free electron masers," *Journal of Infrared, Millimeter, and Terahertz Waves*, vol. 41, no. 1, pp. 1-140, 2020.

[3] H. Jory, S. Evans, J. Moran, J. Shively, D. Stone, and G. Thomas, "200 kW pulsed and CW gyrotrons at 28 GHz," *International Electron Devices Meeting*, Technical Digest, December 1980, pp. 304-307, Washington, D.C., USA.

[4] H.R. Jory, R.E. Bier, S. Evans, K.L. Felch, L. Fox, H. Hucy, J. Shively, and S. Spang, "First 200 kW CW operation of a 60 GHz gyrotron," *International Electron Devices Meeting*, Technical Digest, December 1983, pp. 267–270, Washington, D.C., USA.

[5] P. Woskoboinikow, "Development of gyrotrons for plasma diagnostics," *Rev. Sci. Instrum.*, vol. 57, no. 8, 2113-2118, 1986.

[6] K. Felch, H. Huey, and H. Jory, "Gyrotrons for ECH applications," *Journal of Fusion Energy*, vol. 9, no. 1, pp. 59-95, 1990.

[7] M. V. Kartikeyan, E. Borie, B. Piosczyk, O. S. Lamba, V. V. P. Singh, A. Mobius, H. N. Bandopadhyay, and M. Thumm, "Conceptual design of a 42 GHz, 200 kW gyrotron operating in the $TE_{5,2}$ mode," *International Journal of Electronics*, vol. 87, no. 6, pp. 709-723, 2000.

[8] Ragini Jain and M.V. Kartikeyan, "Design of a 60 GHz, 100 kW CW Gyrotron for plasma diagnostics: GDS-V.01 simulations," *Progress In Electromagnetics Research B*, vol. 22, pp. 379–399, 2010.

[9] M. V. Kartikeyan, G. Singh, E. Borie, B. Piosczyk, and M. Thumm, "Conceptual Design Studies of an 84 GHz, 500 kW, CW Gyrotron," *International Journal of Infrared and Millimeter Waves*, vol. 27, no. 5, pp. 657-670, 2006.

[10] P. Vamshi Krishna, M. V. Kartikeyan, and M. Thumm, "Mode selection and resonator design studies of a 95 GHz, 100 kW, CW Gyrotron," *IEEE International Vacuum Electronics Conference (IVEC)*, February 21-24, 2011, pp. 1–2, Bangalore, India.

[11] Santanu Karmakar, R. Sudhakar, Jagadish C. Mudiganti, R. Seshadri, and M. V. Kartikeyan, "Electrical and Thermal Design of a W-Band

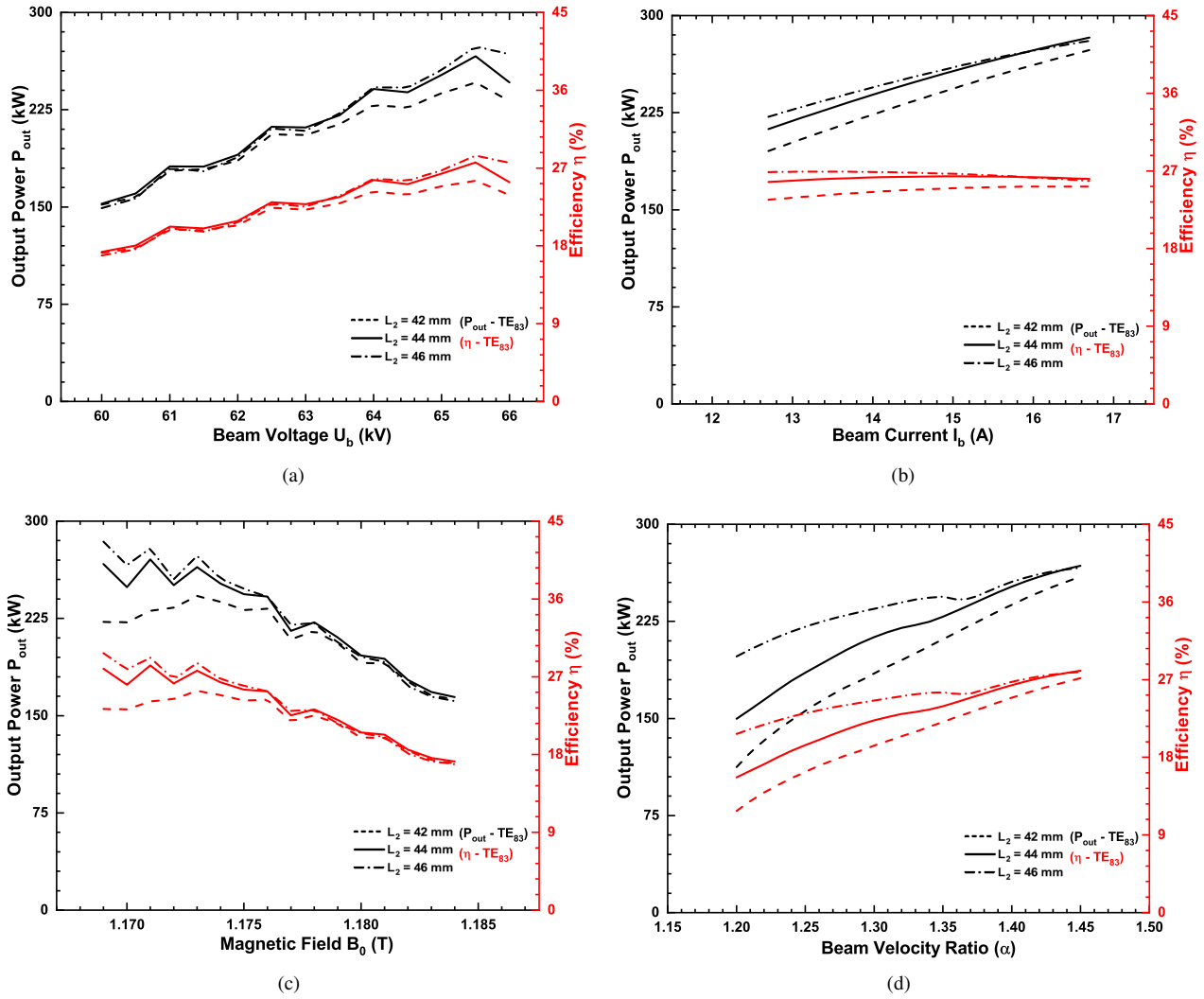

Fig. 7. Plots of output power and efficiency as functions of nominal electron beam parameters at different L_2 for the $TE_{8,3}$ operating mode - medium power operation (a) U_b variation with I_b = 14.7 A, B_0 = 1.174 T, α = 1.4 (b) I_b variation with U_b = 65 kV, B_0 = 1.174 T, α = 1.4 (c) B_0 variation with U_b = 65 kV, I_b = 14.7 A, α = 1.4 (d) α variation with U_b = 65 kV, B_0 = 1.174 T, I_b = 14.7 A.

Gyrotron Interaction Cavity," *IEEE Transactions on Plasma Science*, vol. 47, no. 7, pp. 3155–3159, 2019.

[12] Surbhi Adya, S. Yuvaraj, Santanu Karmakar, M. V. Kartikeyan, and M. K. Thumm, "Investigations on W-Band Second Harmonic Gyrotron for 50/100-kW Operation," *IEEE Transactions on Plasma Science*, vol. 48, no. 12, pp. 4127-4133, 2020.

[13] E. Borie, "Study for second harmonic gyrotrons in the submillimeter region," *International Journal for Infrared and Millimeter Waves*, vol. 15, pp. 311-336, 1994.

[14] P. K. Liu, E. Borie, and M. V. Kartikeyan, "Design of a 24 GHz, 25-50 kW Technology Gyrotron Operating At The Second Harmonic," *International Journal of Infrared and Millimeter Waves*, vol. 21, no. 12, pp. 1917-1943, 2000.

[15] M. V. Kartikeyan, E. Borie, O. Drumm, S. Illy, B. Piosczyk, and M. Thumm, "Design of a 42-GHz 200-kW Gyrotron Operating at the Second Harmonic," *IEEE Transactions on Microwave Theory and Techniques*, vol. 52, no. 2, pp. 686-692, 2004.

[16] Yu Bykov, G. Denisov, A. Eremeev, V. Gorbatushkov, V. Kurkin, G. Kalynova, V. Kholoptsev, A. Luchinin, and I. Plotnikov, "28 GHz 10 kW gyrotron system for electron cyclotron resonance ion source," *Rev. Sci. Instrum.*, vol. 75, no. 5, 1437-1439, 2004.

[17] Anton Malygin, "Design and Experimental Investigation of a Second Harmonic 20 kW Class 28 GHz Gyrotron for Evaluation of New Emitter Technologies," KIT Scientific Publishing, Karlsruhe, Germany, 2016.

[18] D. Borodin, R. Ben-Moshe, and M. Einat, "Design of 95 GHz gyrotron based on continuous operation copper solenoid with water cooling," *Rev. Sci. Instrum.*, vol. 85, no. 7, 074702 (1-8) (2014).

[19] Parth C. Kalaria, "Feasibility and operational limits for a 236 GHz hollow-cavity gyrotron for DEMO," KIT Scientific Publishing, Karlsruhe, Germany, 2017.

[20] C. A. Jain, A. Verma, A. Kumar, M. V. Kartikeyan, E. Borie and M. Thumm, "Design studies of a 460 GHz, 30–50 W, CW second harmonic gyrotron," 2011 IEEE International Vacuum Electronics Conference (IVEC), Bangalore, India, 2011, pp. 59-60, doi: 10.1109/IVEC.2011.5746874.

[21] S. Yuvaraj, Surbhi Adya, D. Mondal, A.S. Thakur, A. Agrawal, M.V. Kartikeyan, and M. Thumm, "GDS2H-V. 2018: A Comprehensive Computer Code Package for the Design of Second Harmonic Gyrotrons," *in Proc. 20th IEEE International Vacuum Electronics Conference (IVEC)*, April 2019, pp. 1-2, Busan, South Korea.

[22] M. I. Petelin, "Self-excitation of oscillations in a gyrotron," *in Gyrotrons: Collected Papers.* Gorki, Russia: USSR Academy Sci., Inst. Appl. Phys., 1981.

[23] K. Kreischer and R. J. Temkin, "Linear theory of an electron cyclotron maser operating at the fundamental," *Int. J. Infrared Millim. Waves*, vol. 1, pp. 195–223, 1980.

[24] G. S. Nusinovich, "Linear theory of a gyrotron with weakly tapered magnetic field," *Int. J. Electron.*, vol. 64, pp. 127–136, 1988.

[25] E. Borie and B. Jödicke, "Comments on the linear theory of the gyrotron," *IEEE Trans. Plasma Sci.*, vol. 16, pp. 116–121, Apr. 1988.